Available online at www.sciencedirect.com
SCIENCE DIRECT®
Fire Safety Journal 40 (2005) 65–78
FIRE SAFETY JOURNAL
www.elsevier.com/locate/firesaf

The transport of water sprays past generic clutter elements found within engine nacelles ☆

Peter J. Disimile[a,*], James R. Tucker[a], Brian Croswell[b], John M. Davis[b]

[a] *USAF 46 Test Wing, Aerospace Survivability and Safety Flight, 2700 D Street, Bldg 1661, Wright-Patterson AFB, OH 45433-7605, USA*
[b] *Department of Aerospace Engineering, UC-FEST Research Group, University of Cincinnati, Cincinnati, OH 45221-0070, USA*

Received 23 July 2003; received in revised form 30 June 2004; accepted 15 August 2004
Available online 23 November 2004

Abstract

The current work is presented as part of an effort to develop a spray transport model that would be used within the computational fire code currently under development by Sandia National Laboratory. As part of a halon replacement research program, new high-boiling-point chemical suppressants have been identified. These agents would discharge in a liquid state and initially result in the transport of liquid droplets through a portion of the nacelle, impinging on various objects prior to reaching the fire zone. The goal of this research effort is to enhance the fundamental knowledge of spray interactions with clutter (e.g., obstacles representing fuel and hydraulic lines, electrical wire bundles, etc). This paper reports on an experimental investigation into the effect of generic cylindrical clutter elements on the performance of a suppressant spray impinging on various clutter densities and porosities. Specifically the amount of agent (water/air spray) that is transported through a generic clutter configuration is presented as a function of clutter spacing and surrounding air. The air coflow speed was set between 0.5 and 6.5 m/s at nominal turbulence levels of 10%.

Keywords: Fire suppression; Engine nacelle; Clutter; Two-phase coflow

☆ This research is part of the Department of Defense's Next Generation Fire Suppression Technology Program, funded by the DoD Strategic Environmental Research and Development Program.
*Corresponding author. Tel.: +1 937 255 6302x212; fax: +1 937 255 2237.
E-mail address: peter.disimile@wpafb.af.mil (P.J. Disimile).

0379-7112/$ - see front matter © 2004 Elsevier Ltd. All rights reserved.
doi:10.1016/j.firesaf.2004.08.003

1. Introduction

Aircraft engine nacelles represent a unique environment for fires and fire protection. Many nacelles are characterized by high air exchange rates and a strong degree of nonuniformity and turbulence within the airflow [1]. In addition, nacelles contain large amounts of plumbing, wiring, avionics and mechanical components mounted on the engine or along the nacelle walls. Some nacelles also have large ribs for structural purposes. This combination of a highly turbulent airflow, flammable fluids, and numerous ignition sources make aircraft engine nacelles a difficult fire zone to protect.

For the past several decades, halogenated agents, notably Halon 1301, have protected engine nacelles. Since the production ban on halon, scientists and engineers in the public and private sectors have been working on replacement agents and new technologies that attempt to replicate Halon 1301's beneficial attributes. Thus far none have succeeded completely. Of the technologies that have been deemed acceptable, based on environmental friendliness, toxicity, materials compatibility, etc. all lack fire-suppression efficiency as measured by weight and/or volume [2].

To improve the fire-suppression efficiency of these candidate technologies, one area of focus is suppressant distribution. Since Halon 1301 was so efficient, research into understanding the engine nacelle airflow offered little payoff. Today, however, a better understanding of the nacelle airflow and how it impacts fires within a nacelle, as well as suppression distribution, can have a large payoff in reducing the design time and/or weight of a halon replacement system.

An additional complication is due to the fact that some halon replacements have a high boiling point, when compared to Halon 1301. These fluids can prove to be especially challenging to distribute in an aircraft engine nacelle. To understand how these systems would perform and thereby optimize a design, engineers must understand better how a cloud of liquid droplets behaves when convecting within a highly turbulent airflow through a cluttered engine nacelle.

Although the current problem may be thought to be related to common two phase flow separation processes (i.e. flow demisters, cooling towers and steam separators) the flow fields in these areas of study differ greatly. In these two phase flow processes the flow fields are typically homogenously droplet laden and impinge on wires or wires meshes smaller than the mean droplet diameter. In the current problem, the drops are two to three orders of magnitude smaller than the elements on which they locally impinge and emanate from a simple concentrated point source at relatively high velocity. Therefore, the common area of two phase flow separation offers little assistance to the current problem.

Earlier studies of spray impingement involved the development of spray to wall interaction models. An example of these studies can be seen in [3]. The term wall indicates that the impacted surface is much larger than the spray jet. Although these studies help in describing and modeling the phenomena of the droplet to wall interactions, they do not provide insight into the effect of solid obstacles of finite dimensions in a coflow regime.

A study involving spray impingement on a solid object in the presence of coflow air was done by Ghielmetti [4]. In this study, Ghielmetti analyzes droplet impacts on a conical surface with an air coflow around a surface. However, the main focus of this study was on secondary droplet behavior (droplets formed after impact), and does not investigate the overall spray interaction in the field either upstream or downstream of the impacted surface.

A more relevant study was conducted by Hung [5] investigating droplet impaction with a cylindrical object of a finite size relatively close to that of the diameter of the droplet, i.e. spray impingement on single wires. This study provides knowledge on how the size of the droplets dripping off wires can be predicted, but again does not include an air coflow and is more focused on the impact phenomena rather than the volume of the spray dripping off the wires.

More recent investigations were done as part of the same NGP program of which the current work is included [6–9]. DesJardin et al. [6] presented a subgrid CFD spray model that could possibly predict the effects of a liquid spray in a cluttered aircraft engine nacelle. However, to the understanding of the authors, this CFD model has only been tested against experimental data for airflow over a single circular cylinder. Another investigation was conducted by Presser et al. [7] predicting a suppressant spray impacting a circular cylinder. This investigation predicted the spray flow field around the cylinder using a numerical model and tested the numerical model with experimental data for fog droplets over a single circular cylinder. The experimental data consists of particle image velocimetry (PIV) velocity measurements of fog injected using a pencil fogger with a specified tight range of drop sizes. Velocity measurements of the fog droplets were taken over a single circular cylinder in the presence of a turbulent coflow. The experimental arrangement of Presser's study is mounted vertically such that the main coflow direction is vertically upward over the cylinder. Both of the above-described studies indicate that further experimental data is needed for verification and modification of their derived models.

DesJardin et al. [8] provides the derivation of a numerical model describing the impact of a 1 mm liquid droplet on a singular circular cylinder. This model is useful in explaining the physics of the liquid droplet impaction on the cylinder and can be used in future models to explain the droplet interaction with the clutter elements. However, this investigation does not include any experimental measurements of spray impingement on a circular clutter element.

The most recent investigation directly related to the current one presents droplet velocity and diameter measurements in the field surrounding a heated cylinder in the presence of a droplet-laden homogenous turbulent flow field [9]. Measurements were taken over both a heated and an unheated cylinder, mainly to highlight the different effects of fire suppressants flowing over structures when heated well above the boiling point of the fire suppressant.

Even though several researchers have investigated various aspects of the current project, experimental research has yet to be done that includes the volume flow of a sprayed suppressant through a multi element clutter in the presence of a turbulent coflow. By finding the dependency of the suppressant volume transported through

clutter as a function the coflow airspeed and clutter density, the amount of suppressant needed to effectively extinguish fires in aircraft engine nacelles can more appropriately be sized. To this end the present study focuses the ability of water drops to pass through a series of cylindrical obstacles, representing generic clutter, while moving in a turbulent coflow.

2. Suppressant spray flow facility $(SF)^2$

A low-speed flow facility with the test section air speed ranging from 0.0 to 12 m/s (0 to 40 ft/s) was modified for the current program. The major components of this facility include an inlet contraction, turbulence generator, test section, clutter section, and the return and separation plenum. A general overview of these components is provided in the following text.

Air drawn from a large laboratory is accelerated towards the test section by a 3.5:1 inlet contraction that serves as the coflow supply. To minimize outside disturbances from propagating directly to the test section, a flow-conditioning unit was placed over the inlet entrance. At the exit of this contraction, a turbulence generation section was also attached. As the coflow exits the turbulence generation section, it enters the test section. The test section was divided into two zones, A and B. Fig. 1 is a digital image of the upstream portion of the facility test section (zone A).

Zone A also contains the suppressant spray nozzle and the clutter package. Zone B represents the remaining portion of the test section which is located downstream of the clutter package. Both zones have a nominal 610 mm × 914 (24″ × 36″) cross sectional area. Zone A is 1220 (48″) in streamwise length, while zone B is 2440 mm (96″) in streamwise length. As previously noted provisions have been made for the insertion of clutter packages at the downstream end of zone A. The leading edge of

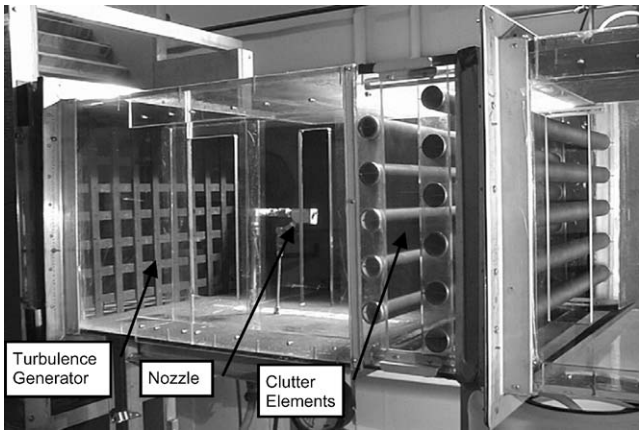

Fig. 1. $(SF)^2$ zone A test section.

the clutter package is held fixed at 952.50 mm (37.50″) from the turbulence generation grid. The exit of the suppressant spray nozzle is located within the coflow, 596.90 ± 0.79 mm (23.50″ ± 0.03″) downstream of the turbulence generation grid. Further the nozzle exit is positioned along the coflow centerline, located 304.80 ± 0.79 mm (12.00″ ± 0.03″) vertically and 457.20 ± 0.79 mm (18.00″ ± 0.03″) horizontally from the test section walls. This also corresponds to the nozzle exit being located 355.60 ± 0.79 mm (14.00″ ± 0.03″) upstream of the leading edge of the clutter package.

Utilizing constant temperature anemometry, velocity surveys at selected streamwise locations within the coflow were performed. Specifically, hot film probes were used to measure the velocity profile within the $(SF)^2$ test section in the absence of any turbulence generating grid, spray nozzle, or clutter package. Fig. 2 displays the results of vertical (y-direction) velocity traverses simultaneously acquired using three hot film probes positioned in zone A, 723.90 ± 0.79 mm (28.50″ ± 0.03″) downstream of the test section inlet, with the coflow air speed set at 5.00 ± 0.25 m/s (16.40 ± 0.82 ft/s). Since the hot film probes were calibrated for each test the maximum error in Fig. 2 was minimized to ±0.1%. These probes were positioned on the centerline ($z = 0$), and at transverse locations, $z = \pm 168$ mm (±6.6 in). The measurement survey was arranged such that the $y = 0$ position corresponded to the vertical center of the test section. Hot film data were acquired at a sampling rate of 1 kHz for a period 20 s, providing 20,000 samples for each spatial location traversed. These data were analyzed and both the time average and standard deviation computed. Results of these surveys indicate that the mean velocity in the streamwise direction over the central portion of the test section (vertical height of 508.00 ± 0.79 mm or 20.00 ± 0.03 in) was 4.75 ± 0.17 m/s. Over the available span of the probe holder (approximately 16 in) the two dimensionality of the coflow was determined to be ±2%. Turbulent intensities (TI) of approximately 1% were also determined at all positions across the $(SF)^2$ test section except close to the walls where boundary layer effects are observed.

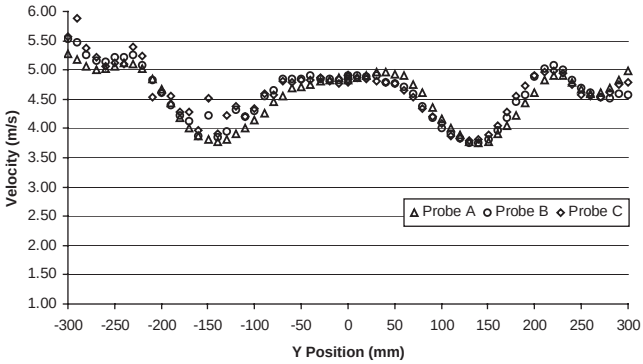

Fig. 2. Streamwise velocity profiles with large grid.

2.1. Turbulence generator

A large grid consisting of several 2.54 mm (1.00 in) wide, 6.35 mm (0.25 in) thick, sharp-edged flat steel slats were assembled in a checkerboard pattern with open cell dimension between the slats of nominally 51 mm × 51 mm (2 in × 2 in). This grid is also visible in Fig. 1. Velocity surveys using hot film probes were acquired downstream of the turbulence generator, at $x = 711.20 \pm 0.79$ mm (28.00 ± 0.03 in), Fig. 2. The spatial locations traversed are identical to those used in the clean test section case. Readily apparent in this figure is the wave-like distribution of the streamwise component of the mean velocity with velocities ranging between approximately 3.7–5.0 m/s (12.0–16.4 ft/s). Although general symmetry can be observed it appears that the lower portion of the test section seemed to have a greater degree of unsteadiness. It is believed that additional unsteadiness was a result of smoke generation supply tubes positioned at the entrance of the inlet contraction. In a similar manner turbulent intensities are plotted in Fig. 3. This figure indicates that the large disturbance grid produced TI levels in the range of 10–14%.

2.1.1. Suppressant spray nozzle

The suppressant spray nozzle used in the present study was a dual-fluid, solid cone nozzle patented by the United States Navy as a *Liquid Atomizing Nozzle,* under the US patent number of 5,520,331. Based on preliminary measurements using a Phase Doppler Anemometer it was decided to reverse the gas liquid entrance locations as opposed to the specifications listed in the patent. The nozzle was installed at the y–z center of Zone A of the test section. This resulted in the centerline of the spray nozzle being positioned tangent to the centerline of the test section. However, the spray nozzle centerline was off center, ejecting its spray at a slight downward angle to the test-section centerline. This caused the spray at the center of the flow to have a nonzero velocity in the V and W directions. From a visual inspection, it can also be seen that the nozzle is slightly oriented in the negative y and positive z directions. Although slight, this misalignment was also confirmed during an examination of the velocity data.

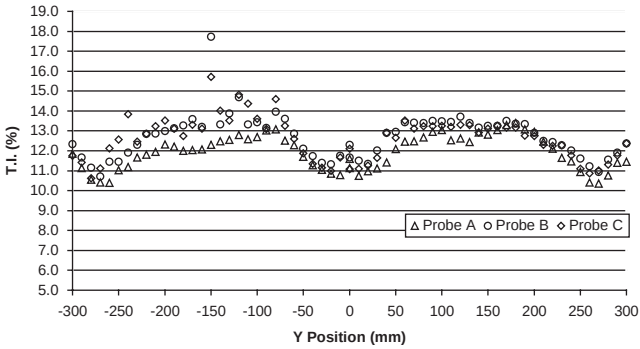

Fig. 3. Streamwise turbulent intensity profiles with large grid.

2.2. Clutter package

The clutter package used in the current test series can be seen installed within zone A of the $(SF)^2$ test section (Fig. 1). The present clutter package consists of 16 two-dimensional elements, spanning the width of the test section. These elements were cylinders and were made from sections of PVC plastic tubing. Elements were assembled to form three separate arrays with equally spaced rows of 5, 6, and 5 tube elements, separated vertically by 42.88 ± 0.79 mm (1.75 ± 0.03 in) between each cylindrical element. The elements have an outer diameter of 50.80 ± 0.79 mm (2.00 ± 0.03 in). The streamwise spacing between each clutter array is variable, ranging from 13.27 mm (0.5 in) to 101.6 mm (4.0 in) with an error of ± 3.175 mm (0.125 in). In terms of element diameter, the spacing ranges from $0.25D$ to $2.00D$ with an error of $0.06D$ (Fig. 4).

The clutter arrangement for this investigation was selected based on its geometric similarity to common elements found within aircraft engine nacelles. It can be seen in Fig. 5 that many cylindrical elements fill the nacelle environment with various local densities. With the capability of varying the streamwise distance between each array of clutter elements in the chosen clutter package, the clutter densities found within larger aircraft engine nacelles is simulated.

2.3. Return and separation plenum

Once the combined coflow air and suppressant mixture exit zone B of the test section, the liquid component must be separated. The separation of the liquid was achieved by first redirecting the flow downward into a recovery pan using a series of turning vanes (see Fig. 6). Upon approaching the liquid pool, already present in the recovery pan the flow is required to make a second, 180 degree turn. Due to the combined mass and high momentum possessed by the liquid drops, the majority of drops are unable to negotiate the tight 180-degree turn, thus impacting the liquid pool. To further minimize suppressant from exiting the return plenum and leaving the flow facility, a 10 μm filter was installed.

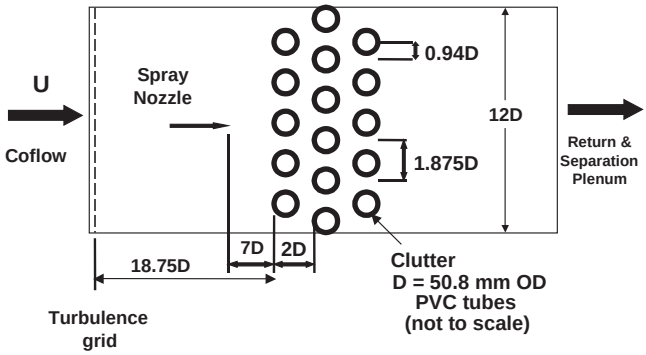

Fig. 4. Sideview schematic of SF^2 test section.

Fig. 5. Typical aircraft engine nacelle clutter.

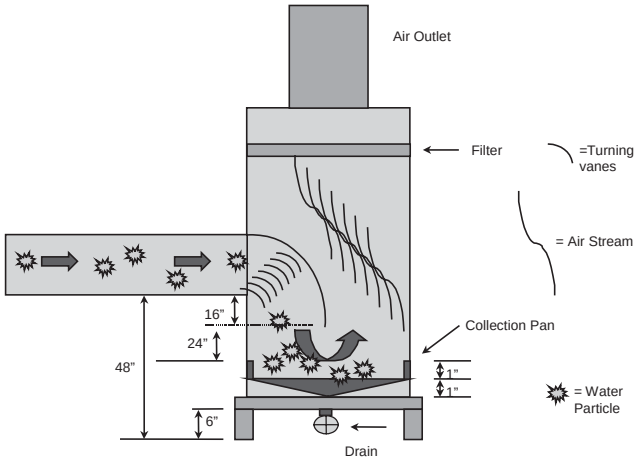

Fig. 6. Side view schematic of SF^2.

2.4. Phase Doppler anemometry system

A three-dimensional phase Doppler anemometer (PDA) was used to acquire the velocity components as well as the diameter of the liquid drops exiting the suppressant spray nozzle. Positioning the measuring volume in the center of the test section required the use of 1000 mm lenses on both the transmitting and receiving optics. In a separate study it was determined, for this measurement configuration the largest spatial filter (Mask A) in the receiving optics was utilized. In this configuration the maximum drop diameter capable of being measured was 810.8 μm.

3. Experimental strategy

The present experimental program utilized a dual-fluid nozzle emitting an air/water spray. This spray was injected into the coflow and allowed to impinge directly on the first array of cylindrical clutter elements. This measurement program was divided into two phases: The first phase documented the transport behavior of a liquid suppressant (water) and its ability to pass through a generic clutter package. While the second phase focused on the measurement of water drop velocities and diameters using the PDA system.

3.1. General strategy

The spray nozzle water flow rate was set and maintained at 17.1 ± 0.4 L/min (4.5 ± 0.1 gal/min) at a corresponding nozzle water pressure of 158.0 ± 13.7 kPa (23.0 ± 2.0 psi). The water flow was monitored using a turbine type flow meter that was positioned directly upstream of a pressure gage. The incoming air was regulated to a pressure of 171.8 ± 3.4 kPa (25.0 ± 0.5 psi). Five different clutter package densities were evaluated during both phases of experimentation. These densities were varied by changes in the streamwise spacing between individual clutter arrays. Array spacing was selected to be $0.25D$, $0.50D$, $1.00D$, $1.50D$, and $2.00D$ with an error of $0.06D$, where D is the diameter of an individual tube. In the current study $D = 50.80$ mm or 2.00 in.

3.2. Phase I: suppressant volume recovery

Experiments were initiated to determine the volume of water transmitted through the clutter package as a function of the streamwise spacing of the clutter array and coflow speed. Thirteen air speeds were investigated ranging from 0.50 ± 0.03 m/s to 6.50 ± 0.33 m/s (1.50 ± 0.08 ft/s to 19.50 ± 0.98 ft/s) in increments of 0.50 m/s (1.60 ft/s). To measure the volume of water passing through the clutter configuration accurately, a repeatable procedure for measuring the liquid water volume was followed. This included the water supply tanks being filled to the same initial starting volume of 303.0 ± 2.8 L (80.0 ± 0.8 gal), the coflow set to the desired speed, and the nozzle air pressure set. A run-time clock was then energized when the water pump was powered on such that the water flow through the nozzle was set to 17.1 ± 0.4 L (4.5 ± 0.1 gal/min). Due to gravity, water drops that wetted the clutter pooled on the individual elements and dripped down into a collection pan located beneath the clutter. Water droplets that passed through the clutter into zone B were deposited within the return plenum. The volume of water that is collected directly under the clutter package was carefully measured, as was the water collected in the return plenum by using graduated containers.

3.3. Phase II: phase Doppler anemometry

PDA measurements were also acquired upstream of the clutter package. At a location in the center of the Zone A test section ($z = 0$) and 2D (101.60 ± 0.79 mm or

4.00 ± 0.03 in) upstream from the leading edge of the clutter package, velocity and diameter traverses were performed. Specifically, the vertical upstream traverses involved PDA measurements at 37 positions (in the y-direction @ $z = 0$) through the center of the water spray. At each location 20,000 data points were acquired. Each vertical location was spatially separated by 3.155 ± 0.022 mm (0.124 ± 0.001 in). The center of the spray nozzle was identified as the location where U, the streamwise component of the mean velocity, reached a maximum, while the lowest Sauter and arithmetic mean diameters were observed. Therefore, the starting and ending position of the traverse could be slightly different depending on this offset, which was within approximately 3.175 to 9.525 mm (0.125–0.375 in). The coflow air speed was maintained at a constant value of 5.00 ± 0.25 m/s (16.40 ± 0.82 ft/s) during PDA measurements. Optimal PDA data acquisition was achieved with a laser power setting of 300 mW.

4. Phase I: suppressant volume results and discussion

Fig. 7 shows the percentage of water recovered directly under the clutter package as a function of element spacing and air speed. The maximum error in the suppressant volume measurements in Fig. 7 varies from ±2% for coflow airspeeds of approximately 0.5 m/s to ±10% at coflow airspeeds of approximately 4.0 m/s. The general trend of the data suggests that the volume of the liquid collected decreases with increasing coflow speed. In fact above 4.5 m/s (~15 ft/s) less than 5% of the liquid is captured and the differences between the five clutter densities diminish. However, with the coflow speed set to 0.50 m/s (1.60 ft/s) the amount of water collected under the clutter ranged from 61.25% ± 0.85% (at 0.25D spacing) to 37.50% ± 0.72% (at 2.00D). As the spacing between the individual clutter arrays is reduced, the amount of water captured increases. Specifically, as the streamwise spacing was reduced from 2.00D to 0.25D, thereby increasing the clutter package density, the water collected increases by over 50%. Data regression using a third

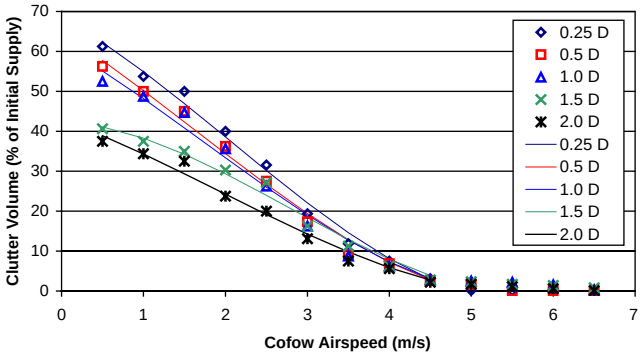

Fig. 7. Clutter recovery vs. airspeed.

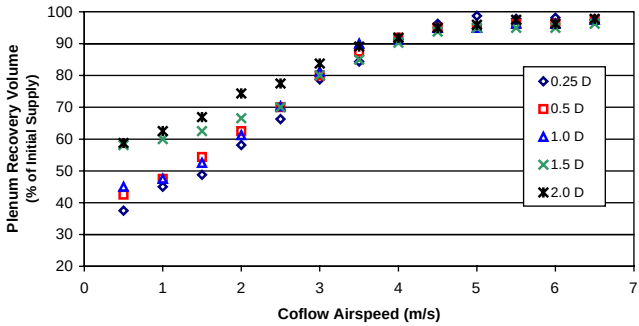

Fig. 8. Plenum recovery vs. airspeed.

degree polynomial was also applied to each clutter-spacing data set and excellent correlation resulted.

Likewise, Fig. 8 indicates the amount of water collected in the return plenum, as function of the coflow speed and clutter spacing. The maximum error for Fig. 8 is $\pm 2\%$ for all data points. All five clutter densities are represented in this figure. The volume in Fig. 8 is also represented as a percentage of the total starting supply volume.

The trends shown in Fig. 8 are the inverse of those seen in Fig. 7. The volume collected in the plenum increases as the coflow airspeed increases. The change in clutter density also has the opposite effect on the plenum recovery volume compared to that of the clutter recovery volume. With the coflow airspeed set to 0.50 m/s the amount of water collected under the clutter ranged from $37.50\% \pm 0.72\%$ (at $0.25D$) to $58.75\% \pm 0.83\%$ (at $2.00D$). The differences between the five clutter spacings also diminish at speeds of approximately 3.5–4.0 m/s and higher. Also it can be seen that the volume recovered in the plenum approaches 100% as the test section speed increases.

During the test evaluation (five clutter spacings and 13 coflow speeds) the percentage of unaccounted water volume between water supply and total liquid recovered was determined. In all cases the difference was random and less than 4%. Due to this small deviation measured in the present study any losses due to evaporation and/or deposition on the tunnel walls can be neglected.

5. Phase II: PDA spray documentation

A velocity vector plot provides an indication of the behavior of the water spray in two-dimensional space. Fig. 9 displays the results of a typical u, v vector plot obtained by traversing across the spray in the y-direction at $x = 254.00 \pm 0.79$ mm (10.00 ± 0.03 in) and $z = 0.00 \pm 0.79$ mm (0.00 ± 0.03 in), when the clutter array X-separation was set to $2.00D$. The drop velocities measured by the PDA system (Fig. 9) have a maximum error of 1%. In general the flow appears to have a symmetric spread with the maximum velocity occurring at the jet centerline. Immediately evident as the water drops exit the nozzle, the drops decelerate in the streamwise

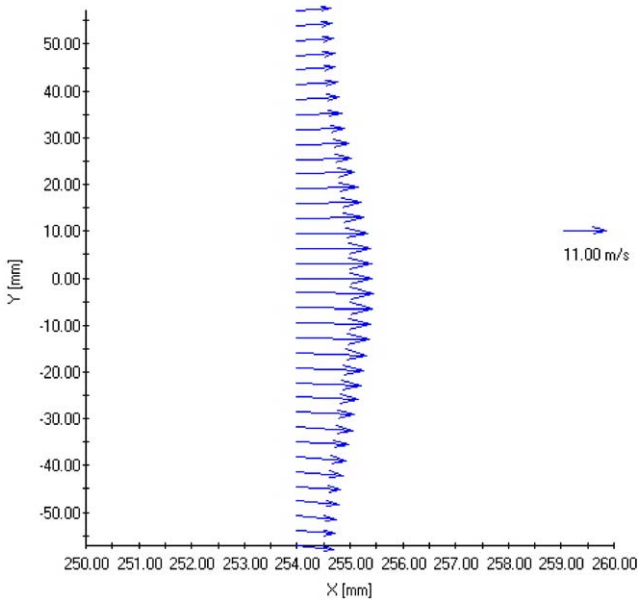

Fig. 9. UV vector plot.

direction and spread in the y-direction. It was determined that the maximum streamwise droplet velocity (U) was approximately 20 m/s (65 ft/s) in the center ($y=0$), decreasing to 9 m/s (30 ft/s) at the edge of the spray. The V component of velocity varied between 1.00 and 2.00 m/s (3.30 and 6.60 ft/s), however, the W component was found to be approximately symmetric around y–z equal zero, varying between -1.00 and $+1.00$ m/s (-3.30 and $+3.30$ ft/s). An examination of these profiles indicated that the spray centerline was pointed downward 0.8 degrees, relative to the $x-z$ plane, which confirmed the visual indication.

The arithmetic mean and Sauter diameter profiles across the center of the jet are shown in Fig. 10. From this figure it can be seen that both the arithmetic and Sauter mean diameter profiles are parabolic in nature. The smallest particles were measured towards the center of the spray. By comparing the diameter and velocity profiles, it can be seen that their diameters are inversely related to the drop velocity. Over the extent of the traverse through the spray, Sauter diameters varied between 285 ± 11 μm at the center of the jet to 350 ± 14 μm at the edge of the jet. All mean diameters in Fig. 10 are within an error of 4%.

6. Summary

To help provide insight into the transport of fire suppressants with high boiling points, an air/-water spray was injected into a highly turbulent coflow of air. Documentation of this coflow at a nominal test section setting of 5.00 m/s verified the presence of a highly

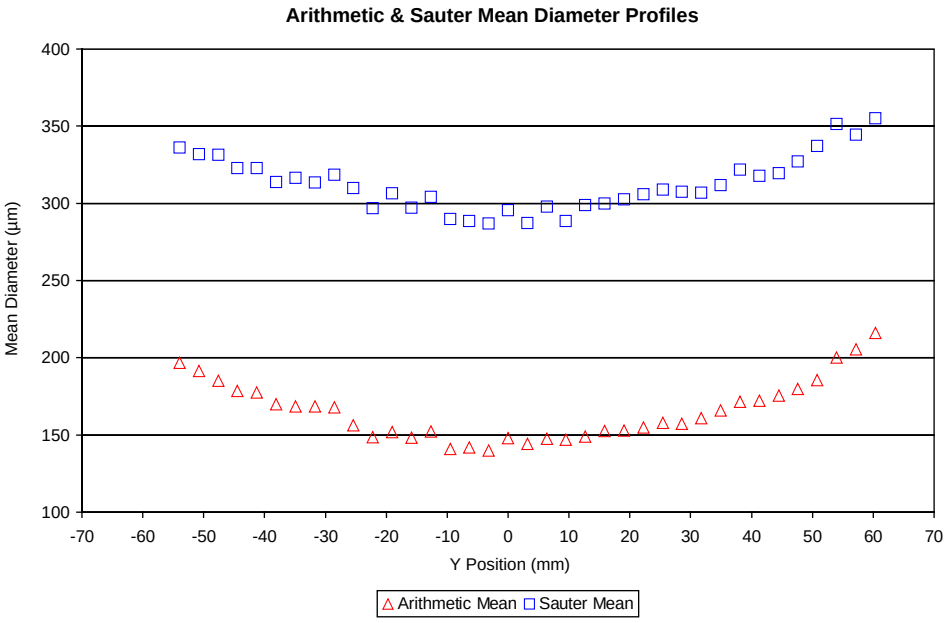

Fig. 10. Mean diameter profiles.

turbulent coflow. Under these conditions the streamwise TI was estimated between 10 and 14% and mean velocity distribution between 3.70 and 5.00 m/s.

Once the nominal boundary conditions were documented, the suppressant volume conservation experiments were performed. This evaluation indicated that, at low coflow airspeeds, as much as 61.25% at 0.25D clutter spacing and 37.50% at 2.00D clutter spacing of the total incoming water supply was collected directly under the clutter element. This corresponded to only 37.50% (at 0.25D) and 58.75% (at 2.00D) of the water volume passing through the clutter package. As a measure of repeatability no less than 96% of the total supply volume was recovered in the combined clutter and plenum return recovery tanks.

The results of this experiment provide valuable insight into the transport of liquid agents through engine nacelles and provide essential data to develop first-generation computer models to aid in the design of fire suppression systems for aircraft engine nacelles. This work however, only addresses round elements of uniform size and distribution. More data are needed to create a database of clutter information for examining the effects of different-size, geometry and density of clutter elements as well as different levels of turbulence.

Acknowledgments

This research is supported by the Department of Defense's Next Generation Fire Suppression Technology Program, funded by the DoD Strategic Environmental

Research and Development Program and monitored by Dr. Richard Gann. The authors would like to thank Dr. Dave Keyser acting on behalf of Naval Air Systems Command for coordinating this activity as well as providing invaluable discussion relating to the experiments. We would also like to thank Mr. Nathaniel McElroy and Veridian Engineering for their technical support in the experimentation.

References

[1] Black AR, Suo-Anttila JM, Disimile PJ, Tucker JR. Numerical predictions and experimental results of air flow in a smooth quarter-scale nacelle. American Institute Aeronautics and Astronautics, Paper AIAA 2002–0856, Virginia, USA; 2002. 16pp.
[2] Grosshandler W, Presser C, Lowe D, Rinkinen W. Assessing halon alternatives for aircraft engine nacelle fire suppression. ASME Trans J Heat Transfer 1995;117:2.
[3] Lee Seong Hyuk, Ryou Hong Sun. Development of new spray/wall interaction model. Int J Multiphase Flow 2000;26:1209–34.
[4] Ghielmetti C. Experimental analysis of a spray impinging on a conical surface. Int J Thermal Sci 2001;40:249–54.
[5] Hung LS, Yao SC. Experimental investigation of the impaction of water droplets on cylindrical objects. Int J Multiphase Flow 1999;25:1545–59.
[6] DesJardin PE, Nelsen JM, Gritzo LA, Lopez AR, Suo-Anttila JM, Keyser DR, Ghee TA, Disimile PJ. Towards subgrid scale modeling of suppressant flow in engine nacelle clutter. Proceedings of the 2001 Halon Options Technical Working Conference; 2001.
[7] Presser C, Widmann JF, DesJardin PE, Gritzo LA. Measurements and numerical predictions of homogeneous turbulent flow over a cylinder: a baseline for droplet-laden flow studies. American Institute Aeronautics and Astronautics, Paper AIAA 2002-0905, Virginia, USA; 2002. 11pp.
[8] DesJardin PE, Presser C, Disimile PJ, Tucker JR. A droplet impact model for agent transport in engine nacelles. Proceedings of the 12th Halon Options Technical Working Conference; 2002.
[9] Presser C, Averdisian CT, Johnson BS. Phase doppler measurements of liquid agent transport over a heated cylinder. Proceedings of the 13th Halon Options Technical Working Conference; 2003.